6th European Conference on Computational Mechanics (ECCM 6)
7th European Conference on Computational Fluid Dynamics (ECFD 7)
1115 June 2018, Glasgow, UK

NUMERICAL SIMULATION OF SUBSONIC GAS FLOWS USING LOCAL DISCRETE NONREFLECTING BOUNDARY CONDITIONS

ILYA V. ABALAKIN[1] **and LUDWIG W. DORODNICYN**[2]

[1] M.V. Keldysh Institute for Applied Mathematics
Miusskaia sq. 4, 125047 Moscow, Russia
ilya.abalakin@gmail.com

[2] M.V. Lomonosov Moscow State University, Faculty CMC
Vorobievy gory, 119991 Moscow, Russia
dorodn@cs.msu.su

Key words: Gas Dynamics, Aeroacoustics, Euler Equations, Artificial Boundaries, Finite Differences, Edge Based Reconstruction

Abstract. This paper is devoted to development of nonreflecting boundary conditions for finite-difference schemes in multi-dimensional gas dynamics. Such boundary conditions are local and do not require large computational resources. The distinction between continuous and discrete formulations is taken into account. Examples of schemes and boundary conditions are shown, which cause small wave reflections for any angle of incidence. Various numerical tests—both linear and nonlinear—are presented.

1 INTRODUCTION

Modeling external problems of subsonic gas dynamics or aeroacoustics faces spurious wave reflections from artificial boundaries. As well known, the multi-dimensional wave equation does not permit local boundary conditions to be transparent for any oblique waves [1]. In fluid dynamics and other fields, alternative techniques are applied such as nonlocal boundary conditions and Perfectly Matched Layers (PML), see, e.g., [2].

In this study a new type of local boundary conditions is developed based on the distinction between continuous and discrete models of fluid dynamics. The latter usually possess additional (singular) modes and require a greater number of equations on boundaries than the continuous do. A typical example is so-called sawtooth spurious waves which are sometimes able to completely destroy the numerical solution.

Henceforth we will examine multidimensional finite-difference schemes as a self-sufficient subject that could not be reduced neither to 1D systems nor to multi-D continuous models. The first do not encounter main difficulties, and the last do not exhibit interesting features. At the same time, the basics will be seen at the level of linearized constant-coefficient equations. This makes applicable simple mathematical tools such as the Fourier–Laplace transform.

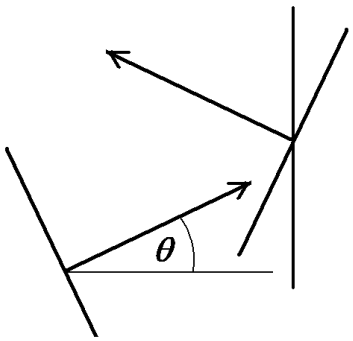

Figure 1: Schematic of wave reflection from the right-hand boundary

The bibliography on discrete nonreflecting conditions is not very extensive. The type of boundary conditions considered here is known, e.g., from [3]–[7]. They are incompatible with the differential systems because of excessive number of equations and, on the other hand, suitable for a chosen finite-difference approximation. Despite the success gained, detailed research of multidimensional numerical models still lacks.

We will analyze and systematize numerical schemes and boundary conditions. There exist formulations resulting in small wave reflections for any angle of incidence.

The theory presented is illustrated with numerical examples both linear and nonlinear, starting from 3-point centered-difference schemes and arriving in high-order 3- and 5-point upwind schemes of EBR (Edge Based Reconstruction) type on unstructured meshes [8].

2 BOUNDARY CONDITIONS FOR DIFFERENTIAL HYPERBOLIC EQUATIONS

2.1 Wave equation

Consider the 2D wave equation in a rectangular domain

$$\frac{\partial^2 p}{\partial t^2} - \left(\frac{\partial^2 p}{\partial x^2} + \frac{\partial^2 p}{\partial y^2} \right) = 0, \quad 0 < x < X, \ 0 < y < Y, \ t > 0. \tag{1}$$

The governing equation is equivalent to the system of acoustic equations

$$\frac{\partial u}{\partial t} + \frac{\partial p}{\partial x} = 0, \quad \frac{\partial v}{\partial t} + \frac{\partial p}{\partial y} = 0, \quad \frac{\partial p}{\partial t} + \frac{\partial u}{\partial x} + \frac{\partial v}{\partial y} = 0. \tag{2}$$

In the 2D case, for the wave equation *nonlocal* nonreflecting boundary conditions are only available. Any local constant-coefficient boundary condition causes reflection of oblique waves (Fig. 1) with a uniquely determined ratio between amplitudes of the incident and the reflected waves.

As an example, set the 1D nonreflecting right-hand boundary condition

$$(\partial p/\partial t + \partial p/\partial x)|_{x=X} = 0. \tag{3}$$

A particular solution to (1) coupled with (3) in the form of plane normal-mode superposition reads

$$\begin{aligned} p(x,y,t;\,\omega,\theta) &= \exp\{i\omega t - i\omega x\cos\theta - i\omega y\sin\theta\} \\ &+ R\exp\{i\omega t + i\omega x\cos\theta - i\omega y\sin\theta\}\,, \qquad R = -\tan^2(\theta/2) = O(s^2)\,. \end{aligned} \tag{4}$$

Here R is the reflection coefficient, θ the angle of incidence, and $s = \sin\theta$.

2.2 Linearized 2D Euler equations

Now turn to the inviscid gas dynamics. Consider the 2D Euler equations in their linearized form

$$\frac{\partial U}{\partial t} + \mathrm{C}_x\,\frac{\partial U}{\partial x} + \mathrm{C}_y\,\frac{\partial U}{\partial y} = 0 \tag{5}$$

expressed in terms of the vector of perturbations $U = (\,\rho'\,u'\,v'\,p'\,)^T$ with constant matrices

$$\mathrm{C}_x = \begin{pmatrix} u & \rho & 0 & 0 \\ 0 & u & 0 & 1/\rho \\ 0 & 0 & u & 0 \\ 0 & \rho c^2 & 0 & u \end{pmatrix}, \quad \mathrm{C}_y = \begin{pmatrix} v & 0 & \rho & 0 \\ 0 & v & 0 & 0 \\ 0 & 0 & v & 1/\rho \\ 0 & 0 & \rho c^2 & v \end{pmatrix}.$$

The general solution to (5) is expanded over normal modes of the four types

$$U(x,y,t;\,\omega,\ell) = \sum_{j=1}^{4} a_j \widehat{U}_j \exp\{i\omega t - ik_j x - i\ell y\}\,.$$

The right-going ($j = 1$) and the left-going ($j = 2$) acoustic waves, the entropy ($j = 3$), and the vorticity ($j = 4$) waves are associated with the following wavenumbers

$$k_1 = \frac{\omega}{c+u}\,, \quad k_2 = -\frac{\omega}{c-u}\,, \quad k_3 = k_4 = \frac{\omega - vl}{u}\,,$$

with acoustic-mode wavenumbers k_1 and k_2 shown for the 1D case, and eigenvectors

$$\begin{pmatrix} \widehat{U}_1 & \widehat{U}_2 & \widehat{U}_3 & \widehat{U}_4 \end{pmatrix} = \begin{pmatrix} \rho & \rho & \rho & 0 \\ c\cos\theta_1 & c\cos\theta_2 & 0 & -c\tan\theta_3 \\ c\sin\theta_1 & c\sin\theta_2 & 0 & c \\ \rho c^2 & \rho c^2 & 0 & 0 \end{pmatrix},$$

$$\tan\theta_j = \ell/k_j\,, \quad j = 1,2,3.$$

For more detail see, e.g., [2].

Consider the right-hand ($x = X$) or the left-hand ($x = 0$) boundary and a boundary condition of general form

$$\mathcal{L}U\big|_{x=x_\Gamma} = 0. \tag{6}$$

From now, we deal with a subsonic rightward-directed flow

$$0 < u < c\,.$$

When so, the left acoustic wave (k_2) propagates leftward as the rest do rightward. Consequently, on the left boundary the right-going acoustic (k_1), the entropy (k_3), and the vorticity (k_4) modes are incoming, when the left acoustic (k_2) is the only outgoing. On the right boundary the waves exchange their properties. Recall that the Euler equations need 3 boundary conditions on the left and 1 condition on the right.

Let $\mathcal{L}$ in (6) be a linear constant-coefficient operator with its Fourier counterpart $\widehat{\mathcal{L}}(k, \ell, \omega)$. In [6] the amplitudes a_j are shown to satisfy the system of linear algebraic equations

$$\sum_{j=1}^{4} \widehat{V}_j a_j = 0\,, \qquad \text{where} \quad \widehat{V}_j = \widehat{\mathcal{L}}(k_j\,, \ell, \omega)\, \widehat{U}_j\,, \quad j = 1, 2, 3, 4.$$

Nonreflecting boundary conditions, by their definition, impose zero amplitudes $a_j = 0$ to incoming waves and arbitrary a_j to outgoing waves. In [6] the *criterion of nonreflecting boundary condition* for the general hyperbolic system is formulated in terms of requirements to matrix columns, i.e., to operator $\mathcal{L}$.
On the right-hand boundary (subsonic outflow) this reads

$$\widehat{V}_1 = \widehat{V}_3 = \widehat{V}_4 = 0\,, \ \widehat{V}_2 \neq 0\,, \quad \forall\, \omega, \ell. \tag{7}$$

On the left-hand boundary (subsonic inflow):

$$\widehat{V}_2 = 0, \quad \widehat{V}_1\,, \ \widehat{V}_3\,, \ \widehat{V}_4 \ \text{ are linearly independent}, \ \forall\, \omega, \ell. \tag{8}$$

In the case of 1D Euler equations these criteria can be easily fulfilled in various ways (see, e.g., [6]). However, in 2D any local boundary conditions does reflect *acoustic* waves to a certain extent. However, there exist boundary conditions for which all entropy and vorticity waves leave the domain with no trace [9].

When switching from linear to nonlinear models, any completely differential (without algebraic terms) boundary conditions can easily be transformed into expressions for the basic variables. We use the following rules:

- in coefficients background parameters are replaced with their local values;

- basic variables are differentiated instead of their perturbations.

The procedure stated above results in exact boundary conditions for the Euler equations in the 1D nonlinear case, as proved in [10] and, more generally, in [6].

3 FINITE-DIFFERENCE GASDYNAMIC SCHEMES

Discrete models considerably differ from continuous ones by the mechanism of wave reflections. In the linear case, this can be explained by the presence of additional modes. As a result, such a numerical scheme requires a greater number of boundary conditions than the initial differential system does. We will construct overdetermined continuous formulations and then discretize them. In some cases this eliminates strong reflections of oblique acoustic waves.

3.1 Schemes for the advection equation

The distinction between differential and finite-difference problems is well seen on the case of three-point centered-difference scheme for the 1D advection equation

$$\partial u/\partial t + \partial u/\partial x = 0\,.$$

It is replaced, on a uniform mesh of size h, with approximation

$$\frac{du_j}{dt} + \frac{u_{j+1} - u_{j-1}}{2h} = 0\,. \tag{9}$$

In a numerical algorithm the time derivative d/dt is implemented by using some Runge–Kutta method.

A normal-mode solution to (9) consists of two parts—the "physical" wave (regular mode) which is similar to the solution of differential equation, and the spurious grid-to-grid (sawtooth) oscillation (singular mode), as below:

$$u(x_j, t) = \exp\{i\omega t - ikx_j\} + R\,(-1)^j \exp\{i\omega t + ikx_j\}\,,$$
$$k = k(\omega, h) = \arcsin(\omega h)/h \approx \omega.$$

Eq. (9) requires boundary conditions at the left edge of the segment and, unlike the continuous advection equation, at the right edge. Here the equation with one-sided difference is commonly used that specifies the reflection coefficient R as

$$\frac{du_N}{dt} + \frac{u_N - u_{N-1}}{h} = 0, \qquad R \approx -\frac{\omega^2 h^2}{4}\,.$$

Yet another, and little more complex, example is the centered-difference scheme with diffusion

$$\frac{du_j}{dt} + \frac{u_{j+1} - u_{j-1}}{2h} = \mu\,\frac{u_{j-1} - 2u_j + u_{j+1}}{h^2}\,. \tag{10}$$

As its simplified version having the same number of modes and boundary conditions may serve the differential convection-diffusion equation

$$\frac{\partial u}{\partial t} + \frac{\partial u}{\partial x} = \mu\,\frac{\partial^2 u}{\partial x^2}\,. \tag{11}$$

The general normal-mode solution to both Eqs. (10) and (11) has the form

$$u(x, t) = a_1 \exp\{i\omega t - ik_1 x\} + a_2 \exp\{i\omega t - ik_2 x\}\,.$$

In the case of convection-diffusion equation (11) the wavenumbers are

$$k_1 = \frac{i}{2\mu}\left(1 - \sqrt{1 + 4i\mu\omega}\right) = \omega - i\mu\omega^2 + O(\mu^2)\,,$$
$$k_2 = \frac{i}{2\mu}\left(1 + \sqrt{1 + 4i\mu\omega}\right) = \frac{i}{\mu} - \omega + O(\mu)\,.$$

The singular mode k_2 is in fact a rapidly dumping exponent.

Discrete scheme (10) has wavenumbers k_1 and k_2 expressed below:

$$\exp\{ik_1h\} = \frac{1}{1+\varepsilon}\left(\varepsilon + ir + \sqrt{1+2ir\varepsilon - r^2}\right), \quad k_1 = \omega - i\mu\omega^2 + O(\mu^2+h^2)\,,$$
$$\exp\{ik_2h\} = \frac{1}{1+\varepsilon}\left(\varepsilon + ir - \sqrt{1+2ir\varepsilon - r^2}\right), \quad k_2 = \frac{i}{h}\ln\frac{\varepsilon+1}{\varepsilon-1} - \omega + O(\mu)\,, \text{ if } \varepsilon > 1,$$
$$k_2 = \frac{\pi}{h} + \frac{i}{h}\ln\frac{1+\varepsilon}{1-\varepsilon} - \omega + O(\mu)\,, \text{ if } \varepsilon < 1; \qquad \varepsilon \equiv \frac{2\mu}{h}\,,\ r \equiv \omega h\,.$$

The singular mode (k_2) of (10) becomes similar to that of (11) when $h \to 0$ with μ kept unchanged and it approaches its properties of centered-difference scheme (9) when $\mu \ll h$.

Finally, consider a scheme with upwind differences used in [8]. The simplest case is the 3-point one-sided scheme which on a uniform mesh has the form

$$\frac{du_j}{dt} + \frac{1}{2h}\Big(3u_j - 4u_{j-1} + u_{j-2}\Big) = 0. \tag{12}$$

and possesses accuracy of $O(h^2)$. This governing equation requires two left boundary conditions and no additional equation on the right.

Scheme (12) has two wavenumbers k_1 and k_2, where

$$\exp\{ik_1h\} = 2 - \sqrt{1-2i\omega h}\,, \quad k_1 = \omega - \frac{1}{3}\omega^3h^2 + O(h^3)\,,$$
$$\exp\{ik_2h\} = 2 + \sqrt{1-2i\omega h}\,, \quad k_2 = -\frac{i}{h}\ln 3 - \frac{1}{3}\omega + O(h)\,.$$

The singular wave is fast-dumping.

3.2 Three-point schemes for the 2D Euler equations

We will deal with a rectangular uniform grid $\{(x_l, y_m)\}$ for mesh sizes Δx and Δy, where linearized Euler equations (5) are approximated on stencils having three points at each coordinate. First consider the centered-difference scheme, like (9),

$$\frac{dU_{lm}}{dt} + \mathrm{C}_x\,\frac{U_{l+1,m} - U_{l-1,m}}{2\,\Delta x} + \mathrm{C}_y\,\frac{U_{l,m+1} - U_{l,m-1}}{2\,\Delta y} = 0\,. \tag{13}$$

Another approximation to Euler equations (5) consists of introducing diffusion into centered-difference scheme (13), see (10), in the following manner:

$$\frac{dU_{lm}}{dt} + \mathrm{C}_x\,\frac{U_{l+1,m} - U_{l-1,m}}{2\,\Delta x} + \mathrm{C}_y\,\frac{U_{l,m+1} - U_{l,m-1}}{2\,\Delta y}$$
$$= \mu\left(\frac{U_{l-1,m} - 2U_{lm} + U_{l+1,m}}{\Delta x^2} + \frac{U_{l,m-1} - 2U_{lm} + U_{l,m+1}}{\Delta y^2}\right). \tag{14}$$

This is a three-point example of the wide-stencil scheme family from [11, 12] with filtering of the basic variables.

A model simpler than the previous is the continuous Euler equations with artificial isotropic diffusion, like (11),

$$\frac{\partial U}{\partial t} + \mathrm{C}_x \frac{\partial U}{\partial x} + \mathrm{C}_y \frac{\partial U}{\partial y} = \mu \left(\frac{\partial^2 U}{\partial x^2} + \frac{\partial^2 U}{\partial y^2} \right). \tag{15}$$

The discretization with respect to y is not important in the further analysis of wave reflections from the left and the right boundaries $x = x_\Gamma$. In Eqs. (13)–(15) first and second y-differences should be replaced by differential operators. Only the mesh in x with size $\Delta x = h$ will be taken into account.

A solution to finite-difference schemes (13)–(15) is expanded over the modes

$$U(x, y, t;\, \omega, \ell) = \exp\{i\omega t - i\ell y\} \left[\sum_{j=1}^{4} a_j \widehat{U}_j \exp\{-ik_j x\} + \sum_{j=1}^{4} a_j^S \widehat{U}_j^S \exp\{-ik_j^S x\} \right].$$

The first four—physical—modes are similar to the correspondent modes featured in continuous Euler equations (5), though they have dissipation and dispersion like in scalar schemes (9)–(11). The rest—singular modes ($\widehat{U}_j^S$, k_j^S)—are strongly model-dependent.

In the case of centered-difference scheme (13) the following relationships take place,

$$\widehat{U}_j^S = \widehat{U}_j\,, \;\; k_j^S = \pm\pi/h - k_j\,, \;\; j = 1, 2, 3, 4.$$

For diffusive Euler equations (15) the expressions are rather complex. When $\mu \to 0$ we obtain the eigenvectors tending to their values from the 1D Euler equations and the asymptotics of wavenumbers,

$$\left(\begin{array}{cccc} \widehat{U}_1 & \widehat{U}_2 & \widehat{U}_3 & \widehat{U}_4 \end{array} \right) = \left(\begin{array}{cccc} \rho & \rho & \rho & 0 \\ c & -c & 0 & 0 \\ 0 & 0 & 0 & c \\ \rho c^2 & \rho c^2 & 0 & 0 \end{array} \right),$$

$$k_j^S = ic_j/\mu\,, \;\; c_j \equiv \omega/k_j\,, \;\; j = 1, 2, 3, 4.$$

Finite-difference scheme (14) does permit analytic formulas for Fourier-analysis, however, very large ones. As a general conclusion, the mode properties are somewhat intermediate between those for systems (13) and (15), as well as in the scalar case (10).

Boundary condition (6) specify the following equation system for amplitudes

$$\sum_{j=1}^{4} \widehat{V}_j a_j = -\sum_{j=1}^{4} \widehat{V}_j^S a_j^S\,, \quad \text{where} \;\; \widehat{V}_j = \widehat{\mathcal{L}}(k_j\,, \ell, \omega)\, \widehat{U}_j\,, \;\; \widehat{V}_j^S = \widehat{\mathcal{L}}(k_j^S, \ell, \omega)\, \widehat{U}_j^S. \tag{16}$$

For all the models (13)–(15), modes k_1, k_3, k_4, and k_2^S propagate rightward, while modes k_2, k_1^S, k_3^S, and k_4^S do leftward, so four boundary equations are needed both on the left and on the right.

We will mean the following concept of nonreflecting boundary conditions for discrete schemes.

- Any kind of incoming waves should not appear if no outgoing wave is present.
- Outgoing *regular* waves should not generate incoming *regular* waves.

This results in the requirements to the solution of Eq. (16):

$$\begin{array}{l} a_j = 0 \ \text{ for incoming modes, } \ \text{if } \forall\, a_l^S \equiv 0, \\ a_j \ \text{arbitrary } \ \text{for outgoing modes.} \end{array}$$

The criterion of nonreflecting condition at the right-hand boundary reads

$$\begin{array}{l} \widehat{V}_2,\ \widehat{V}_1^S,\ \widehat{V}_3^S,\ \widehat{V}_4^S \ \text{ are linearly independent,} \\ \widehat{V}_1 = \beta_{11}\widehat{V}_1^S + \beta_{13}\widehat{V}_3^S + \beta_{14}\widehat{V}_4^S, \\ \widehat{V}_3 = \beta_{31}\widehat{V}_1^S + \beta_{33}\widehat{V}_3^S + \beta_{34}\widehat{V}_4^S, \\ \widehat{V}_4 = \beta_{41}\widehat{V}_1^S + \beta_{43}\widehat{V}_3^S + \beta_{44}\widehat{V}_4^S. \end{array} \tag{17}$$

The criterion for the left-hand boundary reads

$$\widehat{V}_1,\ \widehat{V}_3,\ \widehat{V}_4,\ \widehat{V}_2^S \ \text{ are linearly independent,} \quad \widehat{V}_2 = \beta\widehat{V}_2^S. \tag{18}$$

Above, all the coefficients β may be arbitrary functions of wave parameters. Comparison with the continuous case—(17) vs. (7) and (18) vs. (8)—shows that in both examples the requirements become less restrictive. Local nonreflecting boundary conditions do exist, what will be shown later.

At the left boundary, consider the inflow radiation boundary condition [6] which is nonreflecting for the 1D Euler equations:

$$\frac{d\rho_0'}{dt} + (u-c)\,\frac{\rho_1' - \rho_0'}{h} = 0, \quad \frac{du_0'}{dt} + (u-c)\,\frac{u_1' - u_0'}{h} = 0, \tag{19}$$

$$\frac{dv_0'}{dt} + (u-c)\,\frac{v_1' - v_0'}{h} = 0, \quad \frac{dp_0'}{dt} + (u-c)\,\frac{p_1' - p_0'}{h} = 0. \tag{20}$$

Note that in the continuous case such a system which consists of 4 equations makes the problem setup overdetermined.

The matrices in Eq. (16) are composed of columns

$$\widehat{V}_j = \sigma_j\,\widehat{U}_j\,, \quad \widehat{V}_j^S = \sigma_j^S\widehat{U}_j\,, \quad j = 1,2,3,4,$$

where $\sigma_j \approx i\omega - i\,(u-c)\,k_j$ and $\sigma_j^S \approx \pm 2\,(u-c)/h$. Criterion (18) is fulfilled, where scaling coefficient $\beta = \sigma_2^S/\sigma_2$ and the linear independence is guaranteed because

$$\left(\begin{array}{cccc} \widehat{V}_1 & \widehat{V}_3 & \widehat{V}_4 & \widehat{V}_2^S \end{array}\right) = \mathrm{diag}\,(\sigma_1, \sigma_3, \sigma_4, \sigma_2^S) \left(\begin{array}{cccc} \widehat{U}_1 & \widehat{U}_3 & \widehat{U}_4 & \widehat{U}_2 \end{array}\right).$$

However, the left-going physical wave generates a low-amplitude sawtooth oscillation. System (16) has a particular solution

$$\begin{array}{r} p'(x_j, y, t;\, \omega, \ell) = \exp\{i\omega t - i\ell y\}\left(\exp\{-ik_2 x_j\} + R\,(-1)^j \exp\{ik_2 x_j\}\right), \\ R = O(hs^2). \end{array} \tag{21}$$

The outflow radiation condition [6] on the right-hand boundary

$$\frac{d\rho'_N}{dt} + (u+c)\,\frac{\rho'_N - \rho'_{N-1}}{h} = 0, \quad \frac{du'_N}{dt} + (u+c)\,\frac{u'_N - u'_{N-1}}{h} = 0,$$
$$\frac{dv'_N}{dt} + (u+c)\,\frac{v'_N - v'_{N-1}}{h} = 0, \quad \frac{dp'_N}{dt} + (u+c)\,\frac{p'_N - p'_{N-1}}{h} = 0$$

behaves in similar manner and satisfies criterion (17).

4 NUMERICAL RESULTS

4.1 Propagation of Gaussian acoustic pulse

Consider the propagation of an initial 2D Gaussian pulse in a uniform immovable fluid (Benchmark 3 by [13]). The problem is described by linear acoustic equations (2). The computational domain is square $\{0 \le x \le 50 \times 0 \le y \le 50\}$ with the rectangular uniform mesh of 201×201 nodes.

The governing numerical scheme has the form

$$\frac{\partial U}{\partial t} + \mathrm{C}_x\,\mathcal{D}^h_x U + \mathrm{C}_y\,\mathcal{D}^h_y U = \mu\,\mathcal{F}^h_x U + \mu\,\mathcal{F}^h_y U\,, \tag{22}$$

with vector $U = (\,u\;v\;p\,)^T$ and corresponding matrices C_x and C_y, where

$$\mathcal{D}^h_x u \equiv \frac{1}{\Delta x}\sum_{l=1}^{3} a_l\,(u_{j+l} - u_{j-l})\;, \quad \mathcal{F}^h_x u \equiv \frac{1}{\Delta x}\sum_{l=0}^{3} d_l\,(u_{j+l} + u_{j-l})\;,$$

and the similar operators are applied with respect to y. Parameters a_l and d_l are taken from [11].

For time advancing the explicit 5-stage Runge–Kutta scheme RKo5s by [4] is used.

Three formulations of schemes with boundary conditions were tested.

Case (i). Governing scheme (22) with switched off filtering: $\mu = 0$. Radiation boundary conditions of type (20) are set up at all the four sides of the rectangular domain, e.g.,

$$(\partial u/\partial t + \partial u/\partial x)|_{x=X} = 0, \quad (\partial p/\partial t + \partial p/\partial x)|_{x=X} = 0$$

specified on the right boundary. The spatial derivatives are replaced by biased differences from [7] at 3 rows of near-boundary nodes.

Case (ii). The first equation of governing system (2) and a radiation condition for p, i.e.,

$$(\partial u/\partial t + \partial p/\partial x)|_{x=X} = 0, \quad (\partial p/\partial t + \partial p/\partial x)|_{x=X} = 0,$$

both approximated with biased differences. In the continuous case the problem is well-posed so far as only the second equation is independent.

Case (iii). Governing scheme (22) with filters μ. Radiation boundary conditions like in Case (i).

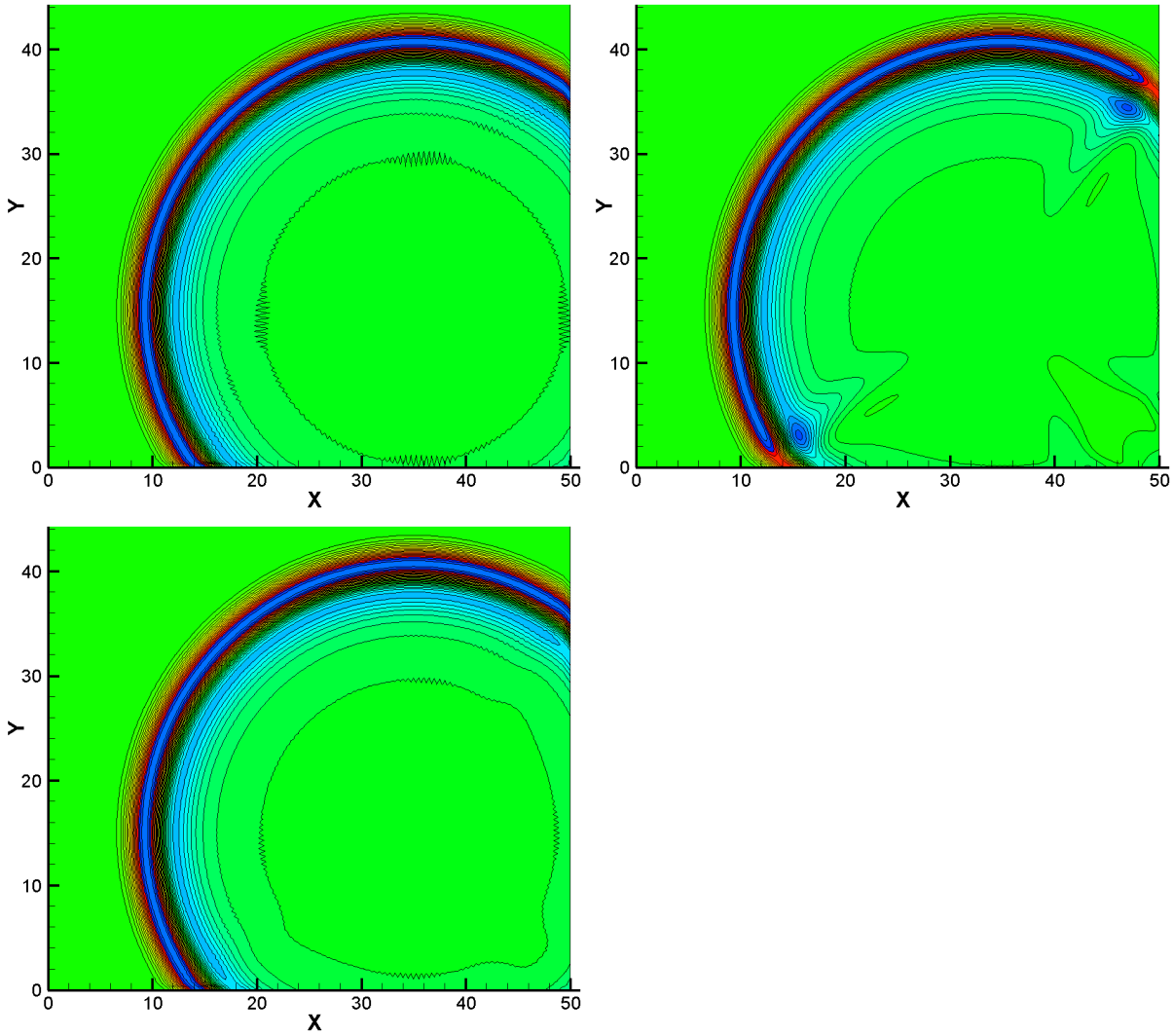

Figure 2: Waves from the initial pulse; top—cases (i) and (ii), bottom—Case (iii)

5 CONCLUSIONS

- For centered-difference schemes, there exist boundary conditions which yield weak reflection of oblique waves with $R = O(hs^2)$.

- For different numerical schemes, same types of boundary conditions cause distinct values of wave reflections.

- The theoretical results in practice can be generalized to more complex models, including wide stencils, nonuniform meshes, and nonlinearity.

REFERENCES

[1] Engquist, B. and Majda, A. Absorbing boundary conditions for the numerical simulation of waves. *Math. Comput.* (1977) **31**:629–651.

[2] Hu, F.Q. On absorbing boundary conditions for linearized Euler equations by a perfectly matched layer. *J. Comput. Phys.* (1996) **129**:201–219.

[3] Tam, C.K.W. and Webb, J.C. Dispersion-relation-preserving finite difference schemes for computational acoustics. *J. Comput. Phys.* (1993) **107**:262–281.

[4] Bogey, C. and Bailly, C. A family of low dispersive and low dissipative explicit schemes for flow and noise computations. *J. Comput. Phys.* (2004) **194**:194–214.

[5] Rowley, C.W. and Colonius, T. Discretely nonreflecting boundary conditions for linear hyperbolic systems. *J. Comput. Phys.* (2000) **157**:500–538.

[6] Dorodnitsyn, L.V. Artificial boundary conditions for numerical simulation of subsonic gas flows. *Comput. Math. Math. Phys.* (2005) **45**:1209–1234.

[7] Dorodnicyn, L.W. Artificial boundary conditions for high-accuracy aeroacoustic algorithms. *SIAM J. Scientific Computing* (2010) **32**:1950–1979.

[8] Abalakin, I., Bakhvalov, P. and Kozubskaya, T. Edge-based reconstruction schemes for unstructured tetrahedral meshes. *Int. J. Numer. Meth. Fluids* (2015) **81**:331–356.

[9] Giles, M.B. Nonreflecting boundary conditions for Euler equation calculations. *AIAA J.* (1990) **28**:2050–2058.

[10] Hedstrom, G.W. Nonreflecting boundary conditions for nonlinear hyperbolic systems. *J. Comput. Phys.* (1979) **30**:222–237.

[11] Tam, C.K.W., Webb, J.C. and Dong, Z. A study of the short wave components in computational acoustics. *J. Comput. Acoustics* (1993) **1**:1–30.

[12] Bogey, C. and Bailly, C. On the application of explicit spatial filtering to the variables or fluxes of linear equations. Short Note. *J. Comput. Phys.* (2007) **225**:1211–1217.

[13] Tam, C.K.W. Benchmark problems and solutions. *ICASE/LaRC Workshop on Benchmark Problems in Computational Aeroacoustics*. NASA CP 3300, Hampton, VA. (1995):1–13.